UDC 621.039.634:621.039.531

LIFETIME ASSESSMENT FOR THE FIRST WALL COMPONENTS OF A FUSION DRIVEN HYBRID NEUTRON SOURCE

V.I. Khripunov

NRC «Kurchatov Institute», Moscow, Russia

A proper simulation of the radiation environment is required to evaluate material performance and structural component exposure times in neutron fields of a fusion-fission hybrid reactor. The relevant neutron and inventory analysis was conducted to quantify the primary radiation damage and radiogenic helium and hydrogen productions in candidate materials (such as Be, W, Cu-alloys, austenitic steels) when used in the first wall of a fusion-fission hybrid. They are greatly influenced by specific features of the combined neutron energy spectrum formed by the two-component neutron source: the fusion neutron source in front of the first wall from the plasma side and the fission neutron source in a subcritical fission blanket behind the first wall. It is shown that the safe subcriticality limit of $k_{\text{eff}} \leq 0.95$ restricts both the neutron and energy multiplications in a hybrid system. Eventually this limit implies that a total neutron fluence of ~10^{23} cm^{-2} may be achieved over the lifetime of a hybrid system. It is more than an order of magnitude lower than what is expected in a DEMO fusion power reactor. Only beryllium as a plasma facing component, should be excluded from further consideration due to the very high He-production in the neutron spectrum of a hybrid reactor, which is largely close to the spectrum of a fast fission reactor. At the same time other materials considered may be used probably during the total operation time of a hybrid reactor.

Key words: fusion-fission hybrid reactor, first wall, material radiation damage.

DOI: 10.21517/0202-3822-2022-45-2-5-14

ОЦЕНКА ВРЕМЕНИ ЖИЗНИ КОМПОНЕНТОВ ПЕРВОЙ СТЕНКИ ТИН С ГИБРИДНЫМ БЛАНКЕТОМ

В.И. Хрипунов

НИЦ «Курчатовский институт», Москва, Россия

Для оценки работоспособности материалов и допустимого времени облучения конструкционных элементов реактора синтеза—деления требуется аккуратное моделирование его радиационных полей. Количественные оценки скоростей образования первичных радиационных повреждений и накопления радиогенного гелия и водорода в материалах-кандидатах для первой стенки гибридного термоядерного реактора, таких как Be, W, медный сплав, вольфрам, аустенитные стали и др., получены по результатам нейтронно-физического и активационного анализа. Показано, что эти процессы в значительной степени предопределяются специфическими особенностями энергетического спектра нейтронов, формируемого двухкомпонентным источником нейтронов синтеза перед первой стенкой (со стороны плазмы) и источником нейтронов деления в подкритическом бланкете с делящимися материалами (за первой стенкой). Показано также, что размножение термоядерных нейтронов и умножение энергии в подкритической гибридной системе ограничиваются предельно допустимым по условиям безопасности значением эффективного коэффициента размножения нейтронов $k_{\text{эф}} \leq 0{,}95$. В конечном счёте этот предел предопределяет и величину полного флюенса нейтронов ~10^{23} см$^{-2}$, который может быть достигнут в материалах первой стенки за всё время эксплуатации гибридной системы. Это значение на порядок величины ниже ожидаемого для энергетического (негибридного) термоядерного реактора ДЕМО. Показано, что только бериллий в качестве компонента, обращённого к плазме, должен быть исключён из дальнейшего рассмотрения из-за высокой скорости образования He в нейтронном спектре гибридного термоядерного источника нейтронов, который в значительной степени близок к спектру ядерного реактора на быстрых нейтронах. В то же время другие рассмотренные материалы могут быть использованы, вероятно, в течение всего срока эксплуатации гибридного реактора.

Ключевые слова: гибридный реактор синтеза—деления, первая стенка, радиационные повреждения материалов.

INTRODUCTION

According to the results of research and development of thermonuclear systems, it is known that high-energy neutrons produced by the deuterium-tritium (D—T)-fusion reactions, when interacting with materials, cause radiation damage to their crystal lattices. Threshold reactions of the (n, α) and (n, p) types lead to formation of the radiogenic He- and H-gas products in materials [1—5]. Ultimately, these two main phenomena, especially the accumulation of radiogenic helium and hydrogen in structural materials, even at low concentrations, have a significant impact on the operational characteristics of the irradiated materials, reducing the service life of the components of a thermonuclear reactor.

Not only the primary D—T-neutrons of a thermonuclear source, but also «secondary» fission neutrons arising in subcritical blankets with fissile materials can also cause additional radiation damage and material transmutations in fusion-driven neutron sources and fusion-fission hybrid reactors, thereby having a significant impact on their structural properties [6—11].

In this paper, it is shown that the fusion neutron multiplication in a subcritical blanket with fission nuclides, accompanied by energy multiplication, is limited by the permissible under safety conditions value of the effective neutron multiplication factor $k_{\text{eff}} \le 0.95$, and by the specific energy release in materials.

It is these limitations that predetermine the total neutron fluence value, radiation damage and radiogenic gases production and accumulation in materials that can be achieved during the entire operation of a fusion-fission hybrid system with a fission blanket.

On the basis of the improved modern computational tools and theoretical models, the maximum values of the radiation characteristics of various materials have been reevaluated, allowing their long-term use in the first wall construction of a fusion neutron source (FNS) with a hybrid blanket.

TWO-COMPONENT NEUTRON SOURCE

As noted in [10], in any hybrid system there are two types of neutron sources simultaneously: a D—T (14.1 MeV) FNS in the plasma zone and a source of fission neutrons with an average energy of ~2 MeV in a subcritical blanket with fissile materials behind the first wall (FW) of the plasma chamber (fig. 1).

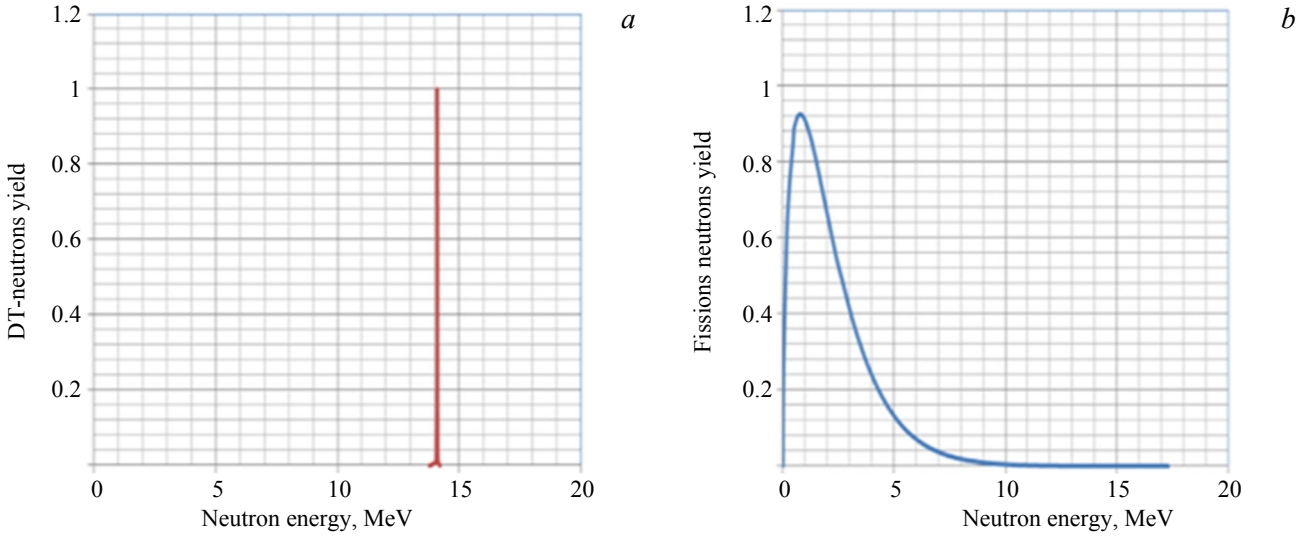

Fig. 1. Neutron source spectra in the DEMO-FNS FW-region [10] with a subcritical blanket: 1 fusion neutron (14.1 MeV) (*a*) and 20 fission neutrons (at $k_{\text{eff}} \le 0.95$) (*b*)

A necessary condition for the nuclear safety of FNS with a hybrid blanket is its subcriticality. It is generally assumed that in any possible conditions for the use of FNS, including new fissile nuclide production in its blanket or fissile actinides burning, the possible reactivity effects with temperature changes or loss of coolants, the effective neutron multiplication factor in the blanket with fissile materials k_{eff} should not exceed 0.95. It is known that in the point approximation, the multiplication of the fission neutrons in a subcritical blanket can be expressed as

$$M_{n\text{-fiss}} = 1/(1 - k_{\text{eff}}), \tag{1}$$

where k_{eff} is the effective neutron multiplication factor resulting from the (n, f)-reactions in the core (i.e. a «fission» blanket zone).

Such an estimate does not take into account the spatial and energy distributions of the fission neutrons, as well as other $(n, 2n)$ and $(n, 3n)$ neutron multiplication reactions. Nevertheless, for further consideration, the value of the neutron multiplication factor $M_{n\text{-fiss}}$ of 20 was accepted as the maximum possible value for FNS with $k_{\text{eff}} = 0.95$.

The corresponding energy multiplication of the D—T-fusion energy in such a subcritical system can reach the value of ~90 [10].

It should be noted also, that in fact, in existing projects of hybrid systems of varying degrees of elaboration ([7, 11] for burning minor actinides, nuclear fuel and electricity generation) the essential part of neutrons is lost in external systems. In these cases the expected k_{eff} is actually about ~0.8—0.9.

NEUTRON SPECTRA IN THE FW FROM THE COMBINED NEUTRON SOURCE

It is known that the damage and gaseous production rates in materials are largely determined by the details of the energy neutron spectra [10].

Neutron spectra caused by the D—T-FNS in DEMO-FNS [11] plasma chamber, the FNS in the subcritical blanket and the resulting spectrum in the FW-area are shown in fig. 2. The average neutron flux energy $E_{n\ avr}$ is ~0.72 MeV in case of water cooled FW. A higher $E_{n\ avr}$ value of 1.3 MeV is expected in other case of Supercritical CO_2 coolant, but this design option is not fully developed.

Numerical values of neutron- and γ-fluxes, as well as neutron fluence values per one continuous full power operation year (FPY) for the combined neutron source are given in table 1.

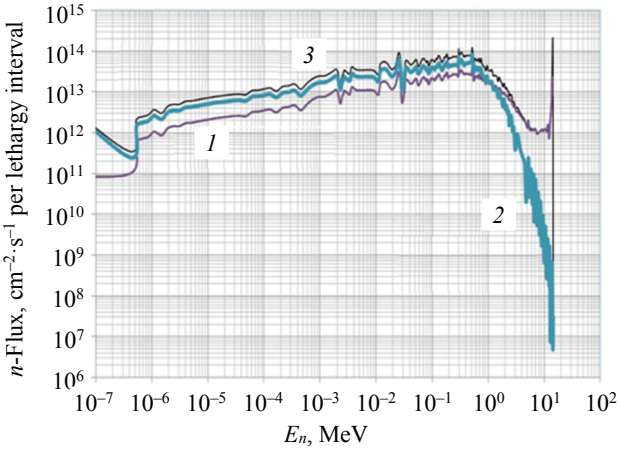

Fig. 2. Neutron spectra in the DEMO-FNS FW-area [11] from the D—T-FNS in the plasma region ($F_{DT\text{-}n}$, at the neutron wall loading of 0.2 MW/m^2) (*1*) and from the FNS in the blanket ($F_{n\text{-}fiss}$ at the neutron multiplication factor of $M_{n\text{-}fiss}$ = 20) (*2*), $F_{DT\text{-}n} + F_{n\text{-}fiss}$ (*3*)

T a b l e 1. **Neutron- and γ-fluxes gamma and neutron fluences in the FNS FW [11] per one FPY for the D—T and FNS**

Fluxes	Neutron flux energy	D—T-fusion neutrons, cm^{-2}·s^{-1}	Fission neutrons, cm^{-2}·s^{-1}	Fission γ-prompt, cm^{-2}·s^{-1}	Total, cm^{-2}·s^{-1}	Total fluence per 1 FPY, cm^{-2}	Total-to-D—T-fusion source ratios
DT-*n*	13.8—14.2 MeV	$1.2\cdot10^{13}$	$4.9\cdot10^{5}$		$1.2\cdot10^{13}$	$3.8\cdot10^{20}$	1.0
n-fast	0.1—13.8 MeV	$6.4\cdot10^{13}$	$7.6\cdot10^{13}$		$1.4\cdot10^{14}$	$4.4\cdot10^{21}$	2.2
n-res	<100 keV	$4.7\cdot10^{13}$	$1.2\cdot10^{14}$		$1.7\ 10^{14}$	$5.3\cdot10^{21}$	3.6
n-th	<0.4 eV	$7.4\cdot10^{12}$	$9.2\cdot10^{13}$		$9.9\cdot10^{13}$	$3.1\cdot10^{21}$	13.4
n-tot	>0	$1.3\cdot10^{14}$	$2.9\cdot10^{14}$		$4.2\cdot10^{14}$	$1.3\cdot10^{22}$	3.3
Gamma		$3.8\cdot10^{13}$	$2.3\cdot10^{14}$	$1.8\cdot10^{13}$	$2.8\cdot10^{14}$	$8.9\cdot10^{21}$	7.4

Whereas the neutron fluence in conventional terms of the neutron wall loading is ~0.2 MW-year/m^2, the integral of the fast neutron flux for one year of continuous operation is $4.4\cdot10^{21}$ cm^{-2}. This is ~2.2 times higher than that from the only single D—T-FNS.

Fig. 3 shows the energy distributions of the neutron flux in the DEMO-FNS FW-area with the two-component neutron source in comparison with the D—T-FNS in the ITER FW-region at the nominal fusion power level of ITER ~500 MW [12].

Additionally, the cumulative distributions of the neutron flux as a function of the upper neutron energy are given in fig. 4 (in relative units). They clearly show an insignificant contribution of thermonuclear (14.1 MeV) neutrons to the energy integral value of the «total» neutron flux in the water-cooled FNS FW compared with the contribution of high-energy neutrons (>0.1 MeV) to the total neutron flux in the ITER FW, also cooled by water.

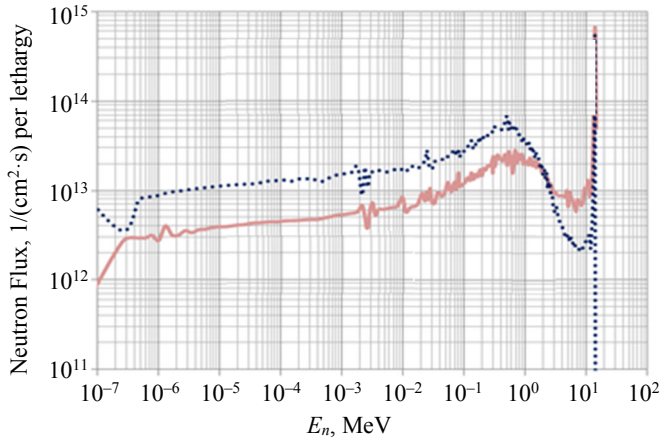

Fig. 3. Neutron spectra in the DEMO-FNS FW and in the ITER FW: ····· — FNS FW, E_n avr = 0.72 MeV; —— — ITER FW, E_n avr = = 3.42 MeV

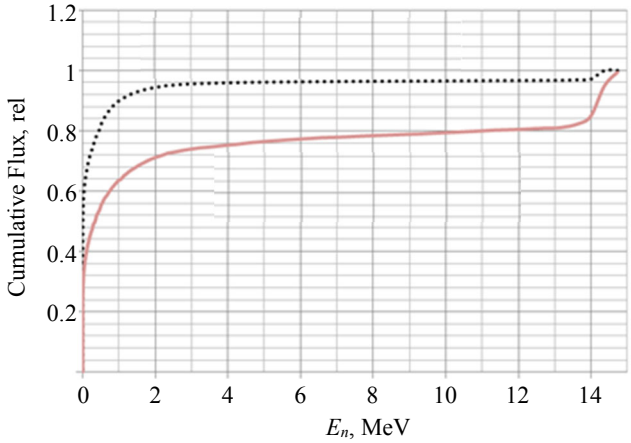

Fig. 4. Cumulative neutron flux f_i ($E < E_n$) to the total neutron flux f_i (tot) ratios for the FNS FW and the ITER FW: ····· — FNS FW, E_n avr = 0.72 MeV; —— — ITER FW, E_n avr = 3.42 MeV

The relative fast neutrons (E_n > 0.1 MeV) fraction in the FNS spectrum is 34% and the intermediate one (E_n = 0.4 eV—0.1 MeV) — ~43%. At the same time the D—T-neutrons (E_n = 14.1 MeV) relative part is only 3%. The thermal neutrons ($F_{n\text{-th}}$) part in case of the water-cooled FW with the beryllium armour is 23% [10].

FW NEUTRON FLUENCES IN THE FNS WITH A FISSION BLANKET AND IN OTHER «PURE» FUSION REACTORS

Radiation damage and other nuclear reactions of the FW-materials are integral characteristics that depend on the cross-sections of nuclear reactions known with different accuracy for neutrons of different energies, and on the duration of irradiation, i.e., on the neutron fluence.

As noted above, the neutron wall loading (in units of MW-years/m^2) is in fact the time-integral current of non-scattered D—T-neutrons. It does not reflect the actual neutron loading on the FW-components under impact of the neutrons from the combined fusion and FNS of a hybrid system. Therefore, it seems appropriate to correlate the responses of radiation exposure to materials to the full neutron energy fluence in units of (cm^{-2}). For comparison, the neutron fluence values expected for some fusion reactors, hybrid reactors and fission reactors are given below.

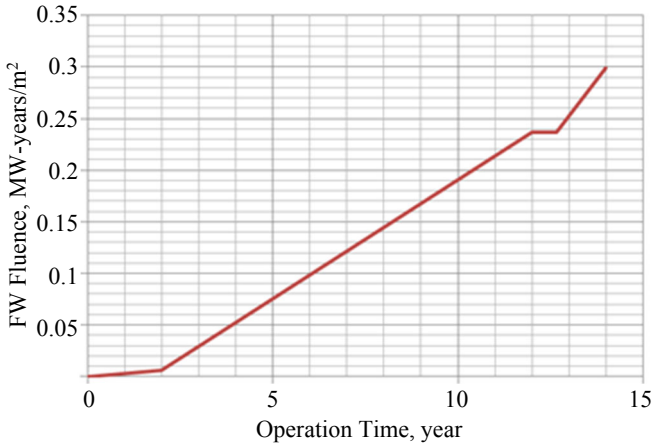

Fig. 5. SA2-scenario of the neutron fluence growth in the ITER FW-area during the «nuclear operation phase» with D—T-plasma [13]

ITER. According to the existing plans for the construction and launch of ITER, its operation in the so-called «nuclear phase» with D—T-reaction source neutrons will take place with gradually increasing thermonuclear power and neutron loading on the FW. The nominal fusion power of 500 MW corresponds to the average neutron wall loading value of 0.56 MW/m^2 and to the total neutron flux value of $1.84\cdot10^{14}$ cm^{-2} [12]. By the end of the ITER operational period, scheduled for about 2049, the total FW neutron fluence according to the SA2 scenario [13] (fig. 5) will reach the maximum value of 0.3 MW-year/m^2 (0.54 Full Power Year) and will be ~$1.7\cdot10^{21}$ cm^{-2}.

It should be noted that this value is two orders of magnitude lower than what is planned to be achieved on the hybrid DEMO-FNS.

EU DEMO. In the European DEMO fusion reactor project [5] with a water-cooled blanket and lithium-lead eutectic as a neutron multiplier and tritium breeder, it is assumed the total neutron flux value will be ~$8.2\cdot10^{14}$ cm$^{-2}\cdot$c^{-1} and the operation period before the blanket replacement will be about 6 years. This corresponds to the neutron fluence value of ~$1.5\cdot10^{23}$ cm^{-2}.

DEMO-FNS. Calculations for the minor actinides burning-out in DEMO-FNS blanket have shown that duration period before the fission blanket reboot can be about 10 years [11]. In terms of the neutron FW loading, the corresponding FW neutron fluence can be ~2 MW-years/m^2, which is typical for some replaceable components of a fusion DEMO [5]. In terms of the FW neutron fluence (from only the D—T-neutron source over 10 years) it can be $4.1\cdot10^{22}$ cm^{-2}, while for the two-component neutron source of the hybrid reactor it is about ~$1.3\cdot10^{23}$ cm^{-2}, which is by 3.2 times higher. It seems that the expected value of neutron fluence is the maximum for the DEMO-FNS with a subcritical blanket.

BN-600. As mentioned earlier in [1] and recently in [14], one of the experimental channels of the BN-600 fast neutron breeder reactor has been used at various times in radiation studies of structural materials for both fission and fusion reactors. It was estimated that at the neutron flux level of ~$6.5\cdot10^{15}$ cm$^{-2}\cdot$s^{-1} in the channel and the irradiation campaign duration of 560 operation days, the neutron fluence reached a value of ~$3.3\cdot10^{23}$ cm^{-2}. This value exceeds the value planned for DEMO-FNS. The average neutron energy $E_{n\text{-avr}}$ in DEMO-FNS is ≤1 MeV for different coolant types. This is comparable to $E_{n\text{-avr}}$ value in the fast breeder BN-600, but significantly lower than the average neutron energy of ~3.4 MeV in the ITER FW-area. The extension of the BN-600

license for operation until 2025 and beyond allows us to hope for a further using this fast fission breeder reactor also for research, development and testing various fusion and hybrid reactor materials.

UNCERTAINTIES IN ESTIMATES OF RADIATION DAMAGE AND GAS PRODUCTION

Due to the emerging possibility of using the FISPACT-II inventory code system [15] for the analysis of radiation damages and material transmutation irradiated by neutrons and charged particles of high energies, that is integrated with the latest TALYS-based TENDL-2017 activation cross sections library [16], it became necessary to re-evaluate the activation characteristics of the DEMO-FNS-materials obtained earlier [10].

Until recently, the FENDL-2.1 (175 energy group) neutron cross sections library was used to evaluate radiation damage in materials caused by neutrons when modeling neutron transport in fusion systems [17]. The radiogenic gas production rates in materials as a result of threshold reactions with high energy neutrons were calculated by applying the EASY-2010 [18] together with the European activation file EAF-2010 [19].

The new system for calculating the activation characteristics of FISPACT-II + TENDL-2017 [15, 16] is distinguished, first of all, by the energy range of incoming neutrons, as well as charged alpha-particles and protons, expanded to 100 MeV, and by the number of energy groups increased to 709 in the library of cross sections of nuclear reactions. This makes it possible to use this integrated system for activation analysis and transmutation of materials, both in fusion and fission reactors and in other devices.

The more detailed group scale is used in the field of thermal neutron energies and the resonance region, which allows for more correct consideration of the so-called blocking of resonant absorption. The latter circumstance is especially important for elements such as tungsten. In total, the neutron energy range from 0 to 15 MeV, characteristic of hybrid thermonuclear systems, accounts for 625 neutron energy groups (with 1175 groups, for example, in [17]).

Recalculation of activation characteristics using the system [15, 16] was performed for materials intended for use in the components of the FW of the DEMO-FNS [20]. The calculation model of the DEMO-FNS FW is a layered system shown in fig. 6.

The first layer facing the plasma is made of beryllium; the intermediate layer is made of chromium-zirconium bronze. Next, the water cooling zone is followed by the zone made of steel or vanadium alloy. Additionally, carbon fiber composite (CFC) and tungsten were also considered as armor materials. The latter is found in most projects of DEMO power reactors not only as a plasma facing component for the FW, but also for the divertors.

The calculated values of radiation damage in units of the number of displacements per atom (dpa) and concentrations of accumulated radiogenic gases in relative units of the number of atoms per million (appm) are given in Table 2.

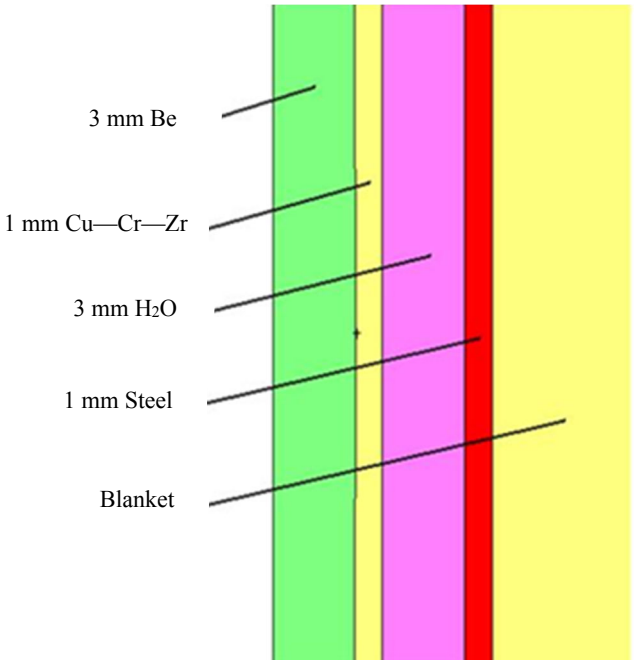

Fig. 6. The layered FW-model of DEMO-FNS

Previous estimates of the primary and secondary radiation damage and radiogenic gas production rates [10], [21], performed by applying the EASY-2010 system [18], FENDL-2.1 [17] cross-section library for neutron transport and European activation file EAF-2010 [10], are marked in Table 2 by the EE index.

New calculation results using the integrated FISPACT-II+TENDL system [15, 16] in the table are marked with the FT index. The results are normalized by the neutron fluence value in the FW-components accumulated over 1 year of continuous operation of the DEMO-FNS. The value is slightly varying in thickness of the FW from $1.30 \cdot 10^{22}$ cm^{-2} on the plasma side to $1.34 \cdot 10^{22}$ cm^{-2} on the blanket side. (In the event that tungsten was considered as the plasma facing material, the fluence value by 1 FPY was somewhat diminished, approximately to $\sim 0.93 \cdot 10^{22}$ cm^{-2} for reason of intensively absorbing moderating neutrons in the resonance energy range.)

Table 2 shows that both inventory code systems, under the same initial conditions, give similar results for calculating radiation damage to materials in units of the number of dpa.

T a b l e 2. **Nuclear responses in the FW-materials from the two-component neutron source in DEMO-FNS (D—T-neutron fluence is ~1.3·10^{22} cm^{-2}/1 FPY) (dpa-primary radiation damage)**

Parameter	Plasma facing materials, Calculation systems					
	CFC		Be		W	
	EE	FT	EE	FT	EE	FT
DPA, dpa	3.2	3.2	2.6	2.6	~0.7	1.4
^{4}He, appm	~230	42	665	666	0.54	0.41
^{3}T, appm	0.03	0.001	28	30	0.005	0.004
^{1}H (+^{2}D), appm	0.24	0.05	1.8	1.8	910	910
	Structure materials, Calculation systems					
	SS316L(IG)		EK-164		V—4Cr—4Ti	
	EE	FT	EE	FT	EE	FT
DPA, dpa	3.1	3.0	3.2	~3.0	3.8	3.9
^{4}He, appm	128	32	160	54	12	12
^{3}T, appm	0.05	0.04	0.01	0.005	0.01	0.01
^{1}H (+^{2}D), appm	139	132	158	141	550	550
	Heat-conducting layer, CuCrZr, Calculation systems					
	EE		FT			
DPA, dpa	3.2		3.0			
^{4}He, appm	22		21			
^{3}T, appm	~0.2		0.16			
^{1}H (+^{2}D), appm	150		180			
	Coolant, H_2O, Calculation systems					
	EE		FT			
DPA, dpa	—		—			
^{4}He, appm	25		47			
^{3}T, appm	0.001		0.001			
^{1}H (+^{2}D), appm	6.6·10^{5} *		6.6·10^{5}*			

*The «burning-out» (transmutation) of hydrogen relative to the value indicated in table 2 is insignificant. In the first case (EE) it is 20 appm, and in the second (FT) case it is ~5 appm.

The exception is tungsten, for which, in the new system [15, 16], based on the results given in [22], in accordance with the generally accepted NRT model of primary damage formation, a lowered threshold energy value causing a displacement of E_d (W) = 55 eV was established [23]. This value was established by computer simulation of cascades based on Binary Collision Approximation by molecular dynamics methods at various empirical potentials and based on the results of experiments performed by Maury et al. [24]. (In previous calculation systems, as well as in the domestic system ACDAM-2.0 [25] E_d (W) was assumed to be equal to 90 eV.)

As for the new estimations for radiogenic helium and hydrogen, which appear in (n, α)- and (n, p)-reactions, respectively, in some cases (like graphite composite and steel), the new estimations of those gas production rates are quite noticeable, almost ~3—5 times less than the previous ones.

This difference seems to be due to the use of the latest version of the TENDL-2017 activation cross-section library, carefully tested on the basis of experiments and carefully coordinated with a number of world libraries of evaluated data.

Due to the noted differences in the estimates of gas formation, as well as a possibility of accounting for the secondary damage caused by charged particles of primary reactions, it seems appropriate to continue using the integrated FISPACT-II + TENDL-2017 to analyze the activation of materials that can be used in hybrid systems with a mixed energy spectrum of fusion and fission neutrons.

The uncertainty in the calculated estimates revealed as a result of the use of various codes and activation cross sections libraries indicates the unreasonableness of using the He appm-to-dpa ratio by some authors as an indicator of the suitability of some installations with different neutron spectra for experiments on fusion materials irradiation. To predict the radiation properties of materials, both separation and integration of damage and gas production effects are important.

THE MAXIMUM OPERATING TIME LIMITED BY PRIMARY RADIATION DAMAGE AND RADIOGENIC GASES ACCUMULATION IN FW MATERIALS

Calculations of primary radiation damage and radiogenic gases accumulation in DEMO-FNS FW with the subcritical blanket were performed using the integrated FISPACT-II+TENDL-2017 system for the materials mentioned earlier in table 2 and for the newly proposed structural materials.

In particular, along with austenitic chromium-nickel steel EK—164 (Fe—16Cr—19Ni—2Mo—2Mn—Nb—Ti—B), which has already shown its radiation resistance under irradiation in the spectrum of the BN-600 fast fission reactor, less activated nickel-free and manganese based modifications EK—164Mn (Fe—16Cr—20Mn—2Mo—Nb—Ti—B) and EK—164MnW (Fe—16Cr—20Mn—2W—NbTi—B) were proposed by specialists of A.A. Bochvar VNIINM in [14] and [26].

Additionally, the so-called «smart alloy» of tungsten with chromium and yttrium W + 11.4Cr + 0.6Y was included in this list, that is considered as the base material for coatings the plasma-facing surfaces in European projects of a demonstration energy thermonuclear reactor [27].

Calculations of activation and transmutation of the DEMO-FNS FW-materials were performed depending on the duration of the campaign to reach the maximum value of the neutron fluence ~10^{23} cm^{-2} after ~10 years of continuous operation (table 3). For comparison, the results of irradiation of the Be-surface layer on the ITER FW are also given in table 3 [28].

T a b l e 3. **The maximum expected radiation damage (dpa) and radiogenic gas production in the DEMO-FNS FW-materials and in the ITER FW, evaluated using the FISPACT-II and TENDL-2017**

DEMO-FNS FW, materials	$F_{n\text{-tot}}$, cm$^{-2}\cdot$s^{-1}	Fluence, cm^{-2}	Dpa, dpa	^{4}He, appm	^{3}T, appm	^{1}H, appm
Be—TShG—56 (+0.003U, Ulba, KZ) [29]	$4.11\cdot10^{14}$	$1.30\cdot10^{23}$	25.6	6728	396	119
CuCrZr—IG [28]	$4.15\cdot10^{14}$	$1.31\cdot10^{23}$	30.3	213	1.52	1800
EK—164 [28]	$4.24\cdot10^{14}$	$1.34\cdot10^{23}$	29.7	280	0.06	1394
EK—164Mn [28]	— " —	— " —	29.0	216	0.34	736
EK—164MnW [28]	— " —	— " —	29.1	217	0.24	732
V—4Cr—4Ti [28]	— " —	— " —	39.4	79	0.11	1020
Hastelloy c276 [28]	— " —	— " —	31.6	359	0.064	2650
W-pure Plansee [28]	$2.97\cdot10^{14}$	$9.39\cdot10^{22}$	15.1	4.2	0.05	913* + 14
W-Smart-Alloy (W—11.4Cr—0.6) [27]	$2.97\cdot10^{14}$	$9.39\cdot10^{22}$	19.8	58.6	0.05	703*+252
ITER FW Be (3D) [28]	$1.8\cdot10^{14}$	$2.6\cdot10^{21}$	0.71	696	8.9	0.7

*The concentration of ^{1}H, initially represented in the material as an impurity, is marked with asterisk.

The calculations have shown the linear growth of radiation damage and radiogenic gases as a function of neutron fluence value.

This means that their formation occurs on the main components of the materials. The role of secondary, multistage reactions (for example, ^{58}Ni (n, γ) ^{59}Ni (n, α) ^{56}Fe, contributing to the formation of helium in Ni-containing materials, the ^{64}Ni (n, α) and ^{62}Ni (n, α) reactions, manifested during prolonged irradiation of copper or ^{188}Os (n, α) and ^{186}Os (n, α) in the transmutation chains of tungsten) is small at these values of neutron fluence.

CRITICAL CONCENTRATIONS OF RADIOGENIC HELIUM

Not only primary dpa, but also formation and accumulation of radiogenic gases (appm) affect the structural integrity, changes in the thermal and electrical conductivity of structural components. For some time now, M.R. Gilbert, J.-Ch. Sublet et al. [30, 31] raise doubts that the number of displacements per atom (in units of dpa) is a comprehensive design characteristic of the radiation resistance of materials, and emphasize that the formation and accumulation of helium in fusion design materials cannot be ignored.

With the support of experimental studies by T. Yamamoto et al. [32] they have developed a model of embrittlement of materials caused by the accumulation of helium at the grain boundaries of the crystal lattice of materials, the so-called «He-induced grain boundary embrittlement».

The model was suggested to give a conservative estimate for the critical He densities in grains that could lead to the grain-boundary destabilization giving rise to helium embrittlement. Without going into details, we note here that the authors of this model associate the atomic concentration of helium G^{c}_{He} atoms produced through transmutation reactions and accumulated in the crystal body with the critical concentration of helium ν^{c}_{He} at the crystal grains of characteristic linear size a (in μm) and the nuclear density of the irradiated material n (cm^{-3}) by the ratio

$$G^{c}_{He} = 3\nu^{c}_{He} / (an). \quad (2)$$

It was assumed for simplicity that all the crystal grains in the given material have cubic shape, and the total number of Helium atoms N_{He} within a grain of linear size a was find as $N_{He} \approx a^3 n G_{He}$.

The calculated critical concentrations of radiogenic helium accumulated in materials with a characteristic size of the crystal grain size a of 0.5 μm are given in table 4.

T a b l e 4. **Calculated critical helium grain-boundary concentrations ν^{c}_{He}, critical bulk concentrations G^{c}_{He}, assumed linear grain size of 0.5 μm [30, 31]**

Material	ν^{c}_{He}, cm^{-2}	G^{c}_{He}, appm	Ref.	Material	ν^{c}_{He}, cm^{-2}	c G^{c}_{He}, appm	Ref.
Be		385.2	[30]	Mo	$1.96 \cdot 10^{15}$	1833.8	[31]
Fe	$1.08 \cdot 10^{15}$	764.6	[31]	W	$2.71 \cdot 10^{15}$	2582.1	[31]
Cr	$1.07 \cdot 10^{15}$	771.9	[31]	Nb	$2.11 \cdot 10^{15}$	2275.2	[31]
V	$1.41 \cdot 10^{15}$	1172.1	[31]	Ta	$2.22 \cdot 10^{15}$	2399.4	[31]

As can be seen from this table, the G^{c}_{He}, values in table 4 show significant variation between different elements. The highest rate of helium formation and the achievement of a critical value of the volume concentration are expected for beryllium. (It should be recalled that the formation of helium in beryllium is due to the ^{9}Be (n, 2n) 2α-multiplication reaction with a not too high energy threshold of ~1.7 MeV, which actually represents the reaction of the Be-fission into two alpha particles and two neutrons.

As follows from the above estimates, the minimum time to reach the critical concentration of helium in the Be component in the FW under hybrid DEMO-FNS-conditions can be about 7 months when the fluence is reached the value of $\sim 7.5 \cdot 10^{21}$ cm^{-2}. It should be noted that beryllium is not considered as a coating of the FW in EU DEMO projects. As for ITER, the critical value for Be can be reached only by the end of its D—T-nuclear operation phase in ~2045, and therefore one should not expect experimental results on the radiation resistance of materials for DEMO fusion of hybrid reactors.

The highest values of critical helium concentrations and, consequently, the maximum permissible irradiation times (and the allowable neutron fluence) are associated with W and Ta.

As for Fe and other components of steels, the achievement of the He-critical concentrations may become a problem only after ~20—30 years irradiation in DEMO-FNS-conditions, when the number of displacements per atoms can reach the value of ~100 dpa.

Currently, it is believed that embrittlement is possible in irradiated ferritic-martensitic steels allowing up to 100 dpa occurring once the concentration of helium in the balk of the grain approached ~400 appm [32].

All this requires confirmation in experiments, for example, on the BN-600 fast reactor.

CONCLUSIONS

The maximum values of the neutron fluence in a fusion driven neutron source with a hybrid blanket are determined by the condition of its subcriticality ($k_{eff} \leq 0.95$) and can be limited to the value of a $\sim 10^{23}$ cm^{-2}, which is an order of magnitude less than the expected neutron fluence in a fusion power reactor.

The use of the proposed materials for applying in the FW-structure of the hybrid DEMO-FNS is possible for decades, with the exception of beryllium.

Only Be as the plasma-facing component should be excluded from further consideration due to very high He- production in the neutron spectrum of a hybrid reactor, which limits its operation life.

Other materials considered (W, Cu-alloys, and austenitic Steels) may be used probably during the total operation time of a hybrid reactor (~10—20 FPY).

The establishment of maximum permissible values of the primary radiation damage (<100 dpa) and radiogenic gases limits (~400 He appm) in these materials are important already at the stage of choosing design solutions (for example, when using welded joints that allow no more than several He appm).

A fusion-fission hybrid reactor with a subcritical blanket is actually a breeder of fission neutrons the spectrum of which is pretty much close to the spectrum of a fast breeder nuclear reactor.

Therefore, the study of some radiation properties is possible, for example, in the core of the fast nuclear breeder BN-600, for a fairly short period of about a year and a half. That provides a several times higher neutron fluence value than it is expected during the entire operation of a fusion-fission hybrid reactor with a fission blanket.

The author would like to express their sincere appreciation to the NEA Data Bank granted him the FISPACT-II version of the integrated code system and the TENDL-2017 Activation Library.

REFERENCES

1. **Fabritsiev S.A., Pokrovskii A.S., Barabash V.R., Prokofiev Y.G.** Neutron spectrum and transmutation effects on the radiation damage of copper alloys. — Fusion Eng. Des., 1997, vol. 36, p. 505—513.
2. **Simakov S.P., Konobeyev A.Yu., Fischer U., Heinzel V.** Comparative study of survived displacement damage defects in iron irradiated in IFMIF and fusion power reactors. — J. Nucl. Mater., 2009, vol. 386—388, p. 52—55.
3. **Gilbert M.R., Dudarev S.L., Zheng S., Packer L.W., Sublet J.-Ch.** An integrated model for materials in a fusion power plant: transmutation, gas production, and helium embrittlement under neutron irradiation. — Nucl. Fusion, 2012, vol. 52, p. 083019.
4. **Sawan M.E.** Damage parameters of structural materials in fusion environment compared to fission reactor irradiation. — Fusion Eng. Des., 2012, vol. 87, p. 551—555.
5. **Stork D. et al**. Developing structural, high-heat flux and plasma facing materials for a near-term DEMO fusion power plant: The EU assessment. — J. Nucl. Mater., 2014, vol. 455, p. 277—291.
6. **Stacey M. et al**. A subcritical, gas-cooled fast transmutation reactor with a fusion neutron source. — Nucl. Technol., 2005, vol. 150, p. 162—188.
7. **Wu Y. and FDS Team**. Conceptual design of the fusion-driven subcritical system FDS-I. — Fusion Eng. Des., 2006, vol. 81, p. 1305—1311.
8. **Jiang J.** Neutronics analysis of water-cooled energy production blanket for a fusion–fission hybrid reactor. — Fusion Eng. Des., 2010, vol. 85, p. 2115—2119.
9. **Siddique M.T., Hong S.-H., Kim M.H.** Physical investigation for neutron consumption and multiplication in fusion–fission hybrid test blanket module. — Fusion Eng. Des., 2014, vol. 89, p. 2679—2684.
10. **Khripunov V.** First wall material damage induced by fusion-fission neutron environment. — Fusion Eng. Des., 2016, vol. 109–111, p. 7—12.
11. **Shpanskiy Yu.S. and the DEMO-FNS Project Team**. Progress in the design of the DEMO-FNS hybrid facility. — Nucl. Fusion, 2019, vol. 59, 076014; https://doi.org/10.1088/1741-4326/ab14a8.
12. **Iida H., Petrizzi L., Khripunov V., Federici G., Polunovskiy E.** Nuclear Analysis of Some Key Aspects of the ITER Design with Monte Carlo Codes. — Fusion Eng. Des., 2005, vol. 74, p. 133—139.
13. **Loughlin M.J., Taylor N.** Recommended Plasma Scenarios for Activation Calculations. — ITER Organization, IDM Number: ITER D 2V3V8G, 2009, v 1.1.
14. **Blokhin A.I., Chernov V.M.** Nuclear physical properties of austenitic nickel and manganese steels under neutron irradiation in nuclear fission (fast) and fusion reactors. — Prob. At. Sci. Technol. Ser. Thermonuclear Fusion, 2020, vol. 43, № 3, p. 11—23.
15. **Fleming M., Stainer T., Gilbert M. et al.** The FISPACT-II User Manual. — UKAEA-R(18)001, 2018.
16. **Koning A.J., Rochman D., Sublet J.Ch.** TENDL-2017: TALYS-based Evaluated Nuclear Data Library (release date December 30, 2017); https://tendl.web.psi.ch.
17. **Aldama D.L., Trkov A.** FENDL-2.1, update of an evaluated nuclear data library for fusion applications. Report INDC (NDS)-467, International Atomic Energy Agency, 2004.
18. **Forrest R.A.** The European Activation System: C07, Overview, EASY Documentation Series. — UKAEA Fus 533, EURATOM/UKAEA Fusion Association the EASY-2010 Software NEA-1564/15, 2007.
19. **Packer L.W., Sublet J.-Ch.** The European activation file: EAF-2010 Biological, Clearance and Transport Libraries. — EASY Documentation Series CCFE-R (10) 04, EURATOM/CCFE Fusion Association, Culham Science Centre, Abingdon, Oxfordshire OX14 3DB, UK, 2010.
20. **Zhirkin A.V. et al.** Assessment of radiation damage to the first wall of a thermonuclear neutron source DEMO-FNS with a blanket for minor actinides transmutation. — Report at the Meeting, NRC «Kurchatov Institute», 15—16 Feb. 2021.
21. **Khripunov V.** Secondary radiation damage and gas production in plasma facing materials under fusion neutron irradiation. — Fusion Eng. Des., 2017, vol. 124, p. 371—375.
22. **Mason D.R., Yi X., Kirk M.A., Dudarev S.L.** Elastic trapping of dislocation loops in cascades in ion-irradiated tungsten foils. — J. Phys.: Condens. Matter, 2014, vol. 26, 375701; doi: 10.1088/0953-8984/26/37/375701.

23. **Bukonte L., Djurabekova F., Samela J., Nordlund K., Norris S.A., Aziz M.J.** Comparison of molecular dynamics and binary collision approximation simulations for atom displacement analysis. — Nuclear Instruments and Methods in Physics Research B, 2013, vol. 297, p. 23—28.
24. **Maury F., Biget M., Vajda P.** Lucasson A. and Lucasson P. Frenkel pair creation and stage (a) recovery in W crystals irradiated near threshold. — Radiat. Eff., 1978, vol. 38, p. 53—65; http://dx.doi.org/10.1080/00337577808233209.
25. **Blokhin A.I., Demin N.A., Manokhin V.N., Sipachev I.V., Blokhin D.A., Chernov V.M.** Software package ACDAM-2.0 for investigation of nuclear physical properties of materials in conditions of neutron irradiation. — Prob. At. Sci. Technol. Ser. Mater. Sci. and New Materials, 2015, vol. 82, p. 81—109.
26. **Chernov V.M., Leonteva-Smirnova M.V. et al.** Structural materials for fusion power reactors — the RF R&D activities. — Nucl. Fusion, 2007, vol. 47, p. 839—848.
27. **Klein F., Litnovsky A. et al.** Smart alloys as armor material for DEMO: Overview of properties and joining to structural materials. — Fus. Eng. Design, 2021, vol. 166, p. 112272.
28. **Barabash V. et al.** Chemical composition and some properties of materials for the ITER in-vessel components for type B radioactive waste assessment. — IDM: ITER_D_2DKPK7 v1.3, 2010.
29. **Kolbasov B.N., Khripunov V.I., Biryukov A.Yu.** On use of beryllium in fusion reactors: resources, impurities and necessity of detritiation after irradiation. — Fusion Eng. Des., 2015, vol. 109—111, p. 480—484.
30. **Gilbert M.R., Sublet J.-Ch.** Neutron-induced transmutation effects in W and W-alloys in a fusion environment. — Nucl. Fusion, 2011, vol. 51, p. 043005; doi: 10.1088/0029-5515/51/4/043005.
31. **Gilbert M.R., Dudarev S.L., Zheng S., Packer L.W., Sublet J.-Ch.** An integrated model for materials in a fusion power plant: transmutation, gas production, and helium embrittlement under neutron irradiation. — Nucl. Fusion, 2012, vol. 52, p. 083019; doi: 10.1088/0029-5515/52/8/083019.
32. **Yamamoto T., Odette G.R., Kishimoto H., Rensman J.W., Miao P.** On the effects of irradiation and helium on the yield stress changes and hardening and non-hardening embrittlement of ~8Cr tempered martensitic steels: compilation and analysis of existing data. — J. Nucl. Mater., 2006, vol. 356, p. 27—49.

Владимир Иванович Хрипунов, в.н.с., к. техн. н., лауреат премии им. И.В. Курчатова, ветеран атомной энергетики и промышленности; НИЦ «Курчатовский институт», 123182 Москва, пл. Академика Курчатова 1, Россия
Khripunov_VI@nrcki.ru

Статья поступила в редакцию 15 января 2022 г.
После доработки 16 марта 2022 г.
Принята к публикации 25 марта 2022 г.
Вопросы атомной науки и техники.
Сер. Термоядерный синтез, 2022, т. 45, вып. 2, с. 5—14.